Taylor & Francis
Taylor & Francis Group

Numerical Heat Transfer, Part A: Applications
An International Journal of Computation and Methodology

ISSN: 1040-7782 (Print) 1521-0634 (Online) Journal homepage: https://www.tandfonline.com/loi/unht20

Effect of nanofluid on thermo hydraulic performance of double layer tapered microchannel heat sink used for electronic chip cooling

Avinash Kumar, Sujit Nath & Dipankar Bhanja

To cite this article: Avinash Kumar, Sujit Nath & Dipankar Bhanja (2018) Effect of nanofluid on thermo hydraulic performance of double layer tapered microchannel heat sink used for electronic chip cooling, Numerical Heat Transfer, Part A: Applications, 73:7, 429-445, DOI: 10.1080/10407782.2018.1448611

To link to this article: https://doi.org/10.1080/10407782.2018.1448611

NUMERICAL HEAT TRANSFER, PART A
2018, VOL. 73, NO. 7, 429–445
https://doi.org/10.1080/10407782.2018.1448611

Taylor & Francis
Taylor & Francis Group

Effect of nanofluid on thermo hydraulic performance of double layer tapered microchannel heat sink used for electronic chip cooling

Avinash Kumar, Sujit Nath, and Dipankar Bhanja

Department of Mechanical Engineering, National Institute of Technology Silchar, Silchar, Assam, India

ABSTRACT

Thermo-hydraulic performance analysis of a tapered double layer microchannel heat sink (DL-MCHS) is done numerically. Water and Al_2O_3–H_2O nanofluid coolants are used with uniform heat flux at the base of DL-MCHS. Comparatively higher heat transfer and lower pressure drop can be achieved considering temperature dependent thermo-physical properties. An overall performance factor is determined which indicates that though the tapered channel gives better thermal performance than straight channel, it is not always advantageous, if hydraulic performance is also considered, due to the increase in pressure drop penalty. Finally, from optimization study, maximum heat transfer is obtained at tapering factor of 0.32.

ARTICLE HISTORY
Received 15 November 2017
Accepted 27 February 2018

Introduction

Miniaturizations of electronic devices for their growing demand, the power and heat flux are increased tremendously over past decades. Therefore, for high performance of these devices their thermal management is indispensable. The conventional air cooling system was found inadequate in removing excess heat which sparks the development of more innovative chip cooling techniques. Many techniques have been used for thermal management of electronic devices among which liquid cooled microchannel heat sink (MCHS) is very effective in cooling the chip. The purpose is to reduce thermal resistance from chip junction and to keep the temperature of chip surface as low as possible.

The first MCHS was proposed by Tukerman and Pease [1] and they manufactured MCHS by etching micro channel on silicon substrate which was 50 μm wide and 300 μm deep to remove heat flux of 790 W cm^{-2} from very large scale integration (VLSI) chip by passing water through micro channels. After this landmark study, many researchers have contributed in this field to enhance the cooling performance of MCHS. Several significant investigations have been performed by many researchers which can be classified as experimental and numerical study [2–7]. Qu and Mazumdar [6,7] concluded that the Navier–Stokes equation and energy equation can satisfactorily predict the fluid flow and heat transfer characteristics of MCHS. Though MCHS is efficient in removing heat from electronic chip but it has some drawback also. A non-uniform temperature distribution was recognized at chip junction due to higher heat generation which cannot be removed by relatively small amount of coolant. This results in thermal stresses in substrate and chip which reduces their life. For removal of this large amount of heat, coolant velocity can be increased but with an undesirable higher pressure drop which ultimately increases the pumping power. To overcome these drawbacks Vafai and Zhu [8] in 1997, proposed first model of double layer microchannel heat sink (DL-MCHS). They have investigated DL-MCHS with counter current flow arrangement and found that base surface temperature along stream wise direction was lesser than single layer microchannel

CONTACT Dr. Sujit Nath sujitnath2008@gmail.com Department of Mechanical Engineering, National Institute of Technology Silchar, Silchar, Assam 788 010, India.

Nomenclature

A	area (m^2)	***Greek symbols***	
c_p	specific heat ($J\,kg^{-1}\,K^{-1}$)	μ	dynamic viscosity (Pa.S)
d	diameter (m)	ρ	density ($kg\,m^{-3}$)
Eu	Euler number		
H	height of DL-MCHS (m)	***Subscript***	
h	height of channel (m)	f	fluid
$\bar{h}$	mean heat transfer coefficient	in	inlet
k	thermal conductivity ($W\,m^{-1}\,K^{-1}$)	nf	nanofluid
L	length of DL-MCHS (m)	out	outlet
Nu	Nusselt number	p	particle
Pf	performance factor	s	solid
Pr	Prandtl number		

heat sink (SL-MCHS). Also, pressure drop was found to be smaller. After Vafai and Zhu, many researchers have investigated and tried to improve DL-MCHS for enhancement of thermal performance [9–12]. Moreover, many researchers have also been investigated stacked multilayered MCHS [13–16].

The reason of using liquid instead of air in MCHS for both single and double layered was to increase the thermal performance. Deionized water, liquid metals, ethylene glycol, PCM slurry, nanofluids are some coolants used by numerous researchers. Among above mentioned liquid coolants nanofluids are new and were found to be very effective. Many researchers have efficiently utilized nanofluids in SL-MCHS [17–20] and also in DL-MCHS [21–24]. They all concluded that nanofluids enhance the heat transfer rate with minor increment of pressure drop. Peygrambarzadeh et al. [19] investigated experimentally the performance of water based CuO and Al_2O_3 nanofluid in MCHS. They concluded that both nanofluids enhance the cooling effect at the expense of higher pumping power. Moreover, CuO–H_2O is found to be more efficient in cooling than Al_2O_3–H_2O. Tsai and Chein [20] investigated analytically the performance of Cu–H_2O and CNT–H_2O nanofluids in MCHS. They found that, nanofluids augment the cooling performance when the porosity and aspect ratio are less than their optimum value but when porosity and aspect ratio crosses their optimum value the nanofluid did not produce any significant change. On the other hand, Gorji et al. [25] optimized MCHS cooled by different nanofluids using response surface methodology (RSM) analysis. They used Cu, Al_2O_3, Ag, TiO_2 nanoparticles in water and ethylene glycol base fluid. They noted that Ag–H_2O nanofluid shows the best cooling performance. Besides that, many works have already been reported on MCHS using Al_2O_3–H_2O as nanofluid [26–28]. However, using diamond-water as nanofluid, Sakanova et al. [29] measured the performance of MCHS in wavy channel.

Similarly, many researchers have efficiently used nanofluids to enhance the cooling performance of DL-MCHS. Hung and Yan [23] investigated numerically the thermal performance of DL-MCHS with Al_2O_3–H_2O nanofluid. Their study was to reduce the thermal resistance of DL-MCHS by varying the particle volume fraction of nanofluid and geometric parameters of channel. They identified an average improvement in thermal performance of 26% over pure water by using Al_2O_3 (1%)–H_2O nanofluid. Sakanova et al. [21] optimized and compared DL-MCHS and double-side (sandwich) MCHS with water-based Al_2O_3 nanofluid with 1 and 5% nanoparticle volume fraction. They found an enhancement of thermal performance by 17.3 at 5% nanoparticle volume fraction while 10.6 at 1% of nanoparticle volume fraction. Rajabifar [24] also used Al_2O_3–H_2O nanofluid in his numerical study to enhance the thermal performance of DL-MCHS and calculated Nusselt number and Euler number for different configurations. Ahmed et al. [22] investigated experimentally a newly designed sequential triangular DL-MCHS with Al_2O_3–H_2O and SiO_2–H_2O nanofluids. They reported that Al_2O_3–H_2O nanofluid with nanoparticle volume fraction 0.9% showed best cooling effect.

Today, due to great advancement in micro fabrication technology it is easier to manufacture complex microstructure. To take this advantage, many researchers have investigated MCHS with

some complex structures like wavy channel [29], ribs and grooves [30], zig–zag channel [31], pin–fin configuration [32] etc. instead of smooth MCHS. The goal is to reduce the thermal resistance and thus to enhance the thermal performance. In addition, a very novel approach to enhance the thermal performance is by converging or tapering the channel. Some literatures are existing regarding the analysis on fluid flow and heat transfer in MCHS with tapered channel. Hung et al. [33] studied three different geometrical configuration of MCHS namely, single layered, double layered, and tapered channel. They optimized the overall thermal resistance with respect to geometric parameters by using conjugate gradient method. They concluded that the tapered MCHS has the lowest value of overall thermal resistance followed by DL-MCHS and SL-MCHS respectively. Dehghan et al. [34] investigated the fluid flow and heat transfer in MCHS with converging channel in laminar regime. They also found that with the increase in tapering, the convective heat transfer coefficient increases and hence the Nusselt number increases. Osanloo et al. [35] investigated numerically the effect of tapered channel in DL-MCHS in which both the lower and upper channel were tapered and fluid flows in counter direction. They obtained thermal resistance, pressure drop and bottom wall temperature for different convergence angle (2°, 4°, and 6°) and flow rates. They have observed that the performance of DL-MCHS increases with convergence angle, however, with the expense of higher pressure drop. Wong and Ang [36] also investigated numerically the thermo-hydraulic performance of a DL-MCHS with tapered channel using water as coolant.

A few research works on MCHS are also available considering variable thermo-physical properties of fluid. Herwig and Mahulikar [37] investigated the effect of variable thermo-physical property in single-phase incompressible flows through micro-channels. Li et al. [38] investigated numerically the water flow and heat transfer in MCHS with $D_h = 0.333$ and at Re of 101–1,775. They used three different methods namely, inlet property, average property and variable thermal property method to investigate the effect of thermo-physical property variation. It has been found that apparent friction coefficient of both average property and variable thermal property methods is less than that of inlet property method while, heat transfer coefficient and Nusselt number are higher than inlet property method. Finally, they concluded that variable thermal property method is superior in engineering application since it characterizes the actual phenomenon by nature and hence it is much accurate. Therefore, it is clear that by using temperature dependent thermo-physical properties of fluid, the prediction of fluid flow and heat transfer in microchannel will be much accurate. Hence, many researchers have used temperature dependent thermo-physical property of fluid in their study with MCHS [21, 29, 39].

From the brief literature review, it is observed that the main purpose in electronic cooling is to reduce the thermal resistance and to keep the chip surface temperature as low as possible and this purpose can be fulfilled efficiently by MCHS and more effectively by DL-MCHS. It is also observed that nanofluids plays a great role as coolant in electronics cooling and are much effective than air and water. The novel approach of tapered MCHS to enhance the thermal performance is also very effective. But, so far to the best of knowledge of the authors the studies of tapered MCHS for both single and double layered was done only using water as coolant. In the present study thermal-hydraulic performance of DL-MCHS is evaluated using Al_2O_3–H_2O nanofluid as coolant and compared the results with water. To obtain much accurate results, temperature-dependent thermo-physical properties for both water and Al_2O_3–H_2O nanofluid are considered using user define function in ANSYS FLUENT. Moreover, the effects of various parameters namely, tapering factor (TF), Reynolds number, nanoparticle volume fraction (ϕ), nanoparticle diameter (d_p) on DL-MCHS are also studied for both water and Al_2O_3–H_2O nanofluid.

Geometric configuration

Figure 1*a* shows the schematic diagram of computational domain of a tapered DL-MCHS. The DL-MCHS is composed of two layers separated by a solid rib where both the lower and upper microchannels are converging in nature due to tapered in the middle rib. DL-MCHS is a counter flow heat sink where the fluid flows through lower channel in positive z direction and through upper channel in negative z direction. The dimensions of heat sink are $L_x = 10$ mm, $L_y = 10$ mm, and $H = 1.5$ mm. Due

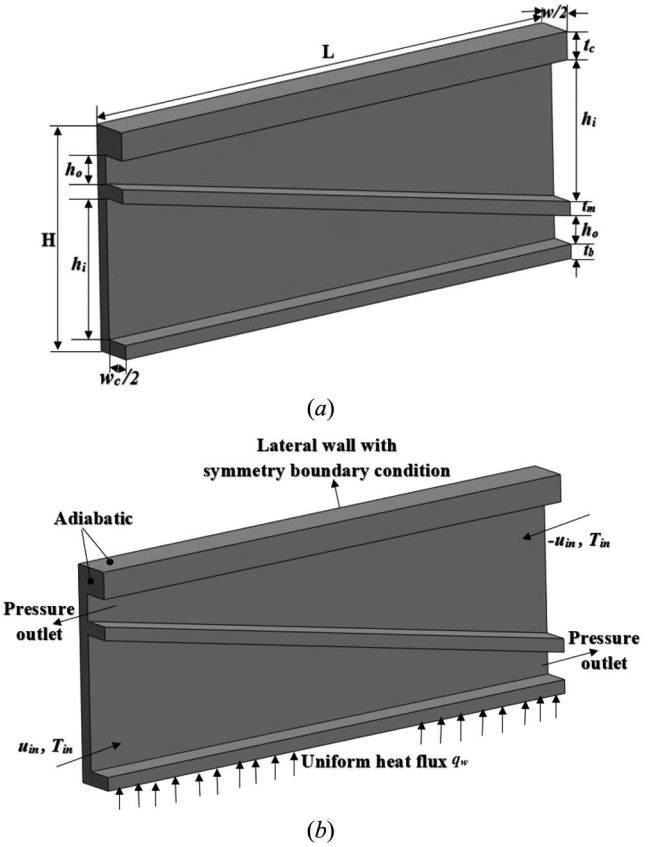

Figure 1. Schematic diagram of computational domain with (*a*) dimensions; (*b*) necessary boundary conditions.

to symmetric body, the computational domain considered is only one lower and upper channel. The dimensions of computational domain are given in Table 1. A heating source like microprocessor chip or VDMOS chip with uniform heat flux q_w, is attached to the bottom wall of DL-MCHS. The DL-MCHS used is made of silicon and the coolant used is water and Al_2O_3–H_2O nanofluid. The thermo-physical properties of silicon and Al_2O_3 are given in Table 2.

Numerical model description

Assumptions and governing equations

A three-dimensional solid–fluid conjugate model is used to investigate the thermo-hydraulic characteristics. The following assumptions are considered.

Table 1. Dimensions of computational domain.

Parameters	Values (μm)
Channel length, L	10,000
Channel width, w_c	50
Channel height at inlet, h_i	Vary with TF
Channel height at outlet, h_o	Vary with TF
Total channel height, $H_c = h_i + h_o$	1,200
Width of computational domain, w	100
Thickness of base, t_b	50
Thickness of middle rib, t_m	50
Thickness of cover, t_c	200

TF, tapering factor.

Table 2. Thermo-physical properties of Silicon and Al_2O_3.

Material	ρ (kg m^{-3})	c_p (J kg^{-1} K^{-1})	k (W m^{-1} K^{-1})
Silicon [30]	2,330	703	149
Al_2O_3 [28]	3,600	765	36

- The fluid flow is single phase, steady state and incompressible flow.
- Radiation heat transfer, gravitational force and thermal contact resistance between the components are neglected.
- The surfaces of the DL-MCHS are well insulated except bottom wall.
- The properties of solid substrate are constant.

Based on above assumptions following governing equations are used:
Continuity equation for fluid:

$$\nabla \cdot \overrightarrow{V} = 0 \tag{1}$$

Momentum equation for fluid:

$$\left(\overrightarrow{V} \cdot \nabla\right)\rho\overrightarrow{V} = -\nabla p + \mu\nabla^2\overrightarrow{V} \tag{2}$$

Energy equation for fluid:

$$\overrightarrow{V} \cdot \nabla T = \frac{k}{\rho c_p}\nabla^2 T \tag{3}$$

Energy equation for solid:

$$k\nabla^2 T = 0 \tag{4}$$

Boundary conditions

The related boundary conditions are given as follows and shown in Figure 1*b*
(A) Inlet boundary condition

$$\text{For bottom channel}: \; u = u_{\text{in}}; v = w = 0\,; T_{\text{in}} = 293\,\text{K} \tag{5}$$

$$\text{For upper channel}: \; u = -u_{\text{in}}; v = w = 0; T_{\text{in}} = 293\,\text{K} \tag{6}$$

(B) Outlet boundary condition
At the exits of both the bottom and upper channels, pressure outlet boundary conditions are specified.

$$(p_{\text{out}})_{\text{bottom}} = (p_{\text{out}})_{\text{upper}} = 1.013 \times 10^5\,\text{Pa} \tag{7}$$

(C) For fluid–solid interface

$$\text{No slip boundary condition on the wall}: \; u = 0 \tag{8}$$

$$\text{No penetration boundary condition}: \; v = w = 0 \tag{9}$$

$$\text{Temperature of fluid and solid are equal}: \; T_{\text{f}} = T_{\text{s}} \tag{10}$$

(D) A uniform heat flux of 100 W cm^{-2} is applied at the bottom surface of DL-MCHS.
(E) The two lateral surfaces of computational domain are taken as symmetry wall boundary condition.
(F) The rest of surfaces of DL-MCHS, i.e., front, back, and top are taken as adiabatic wall.

Temperature dependent thermo-physical properties of water

Initially water is used as coolant and temperature dependent thermo-physical properties of the water are considered as follows [29]:

$$\rho(T) = 1000\left[1 - \frac{T + 15.9414}{508929.2(T - 204.87037)}(T - 276.9863)^2\right] \tag{11}$$

$$c_p(T) = 3908 + 3.826T - 0.01674T^2 + 2.330 \times 10^{-5}T^3 \tag{12}$$

$$k(T) = -1.579 + 0.01544T - 3.515 \times 10^{-5}T^2 + 2.678 \times 10^{-8}T^3 \tag{13}$$

$$\mu(T) = 1.005 \times 10^{-3}\left(T/293\right)^{8.9}\exp[4700(T^{-1} - 293^{-1})] \tag{14}$$

Temperature-dependent thermo-physical properties of Al_2O_3–H_2O nanofluid

The thermo-physical properties of Al_2O_3–H_2O nanofluid are also considered temperature-dependent and the base fluid is water, whose properties are given in Eqs. (11)–(14). The nanoparticles are considered spherical and uniform in shape and size. In present study, density and heat capacity of nanofluid are considered as follows [40]:

- Density

$$\rho_{nf} = (1 - \phi)\rho_f + \phi\rho_p \tag{15}$$

- Specific heat

$$\left(\rho c_p\right)_{nf} = (1 - \phi)\left(\rho c_p\right)_f + \phi\left(\rho c_p\right)_p \tag{16}$$

The thermal conductivity and viscosity of nanofluid are calculated as proposed by Corcione [41]

- Thermal conductivity for nano particle is calculated using Eq. (17) for diameter range 10 nm $\leq d_p \leq$ 150 nm and nano particle volume concentration (ϕ) range of $0.002 \leq \phi \leq 0.09$.

$$\frac{k_{nf}}{k_f} = 1 + 4.4\mathrm{Re}_p^{0.4}[\mathrm{Pr}]_f^{0.66}\left(\frac{T}{T_{fr}}\right)^{10}\left(\frac{k_p}{k_f}\right)^{0.03}\phi^{0.66} \tag{17}$$

where, Re_p is the nanoparticle Reynolds number due to Brownian motion and is given as

$$\mathrm{Re}_p = \frac{\rho_f u_B d_p}{\mu_f} = \frac{2\rho_f k_b T}{\pi\mu_f^2 d_p} \tag{18}$$

where, u_B is the Brownian velocity of nanoparticles and is calculated as the ratio between nanoparticle diameter d_p and the time required to cover a distance without agglomeration $\left(\tau_D = d_p^2/6D\right)$. Where D is Einstein diffusion coefficient, T_{fr} is freezing point of base fluid (273.16 K), T is nanofluid temperature ($294 \leq T$ (K) ≤ 324), k_b is Boltzmann constant (1.38×10^{-23} J K^{-1}) and Pr_f is Prandtl number of the base fluid.

- Viscosity for nanoparticle is calculated using Eq. (19) for diameter range 25 nm $\leq d_p \leq$ 200 nm and nanoparticle volume concentration (ϕ) range of $0.0001 \leq \phi \leq 0.071$.

$$\frac{\mu_{nf}}{\mu_f} = \frac{1}{1 - 34.87(d_p/d_f)^{-0.3}\phi^{1.03}} \tag{19}$$

where d_f is base fluid molecular diameter which is defined as

$$d_f = 0.1\left(\frac{6M}{N\pi\rho_{f0}}\right)^{1/3} \tag{20}$$

where M is molecular weight of base fluid, N is Avogadro number (6.022×10^{23} mol^{-1}), and ρ_{f0} mass density of base fluid at $T_0 = 293$ K.

Computational details

The main focus of the present study is to show the effect of tapered channel on thermal and flow performance of DL-MCHS. Three different tapered channels with tapering factor (TF = 0.801, 0.5, and 0.2) along with straight channel (TF = 1) are investigated for different Re using water and Al_2O_3–H_2O nanofluid as coolant.

The TF is defined as:

$$\mathrm{TF} = \frac{h_o}{h_i} \tag{21}$$

where, h_o is the height of channel at outlet and h_i is the height of channel at inlet as shown in Figure 1*a*. The heights at inlet and outlet of both the bottom and upper channels are equal. And in the present study Reynolds number is defined as:

$$\mathrm{Re} = \frac{\rho_f u_{in} D_{h,in}}{\mu_f} \tag{22}$$

where, $D_{h,in}$ is the inlet hydraulic diameter expressed as:

$$D_{h,in} = \frac{2h_i w_c}{(h_i + w_c)} \tag{23}$$

ρ_f, μ_f, and u_{in} are density, viscosity and inlet velocity of the fluid respectively. The thermal performance of heat sink is evaluated using overall thermal resistance R_{th} proposed by Osanloo et al. [35] as:

$$R_{th} = R_{th,cond} + R_{th,conv} = \frac{L}{k_s A_s} + \frac{1}{h_f A_f} = \frac{T_{max} - T_{min}}{q_w A} \tag{24}$$

where, L is the length of DL-MCHS, k_s is thermal conductivity of substrate, A_s is the heat conduction area, h_f is the convective heat transfer coefficient, A_f is the convective heat transfer area, T_{max} and T_{min} are the maximum and minimum temperature in heat sink, q_w is the heat flux applied at bottom wall, and A is the area at the bottom of heat sink where heat flux is applied. To determine the overall convective heat transfer in the channel having non-uniform cross section, average Nusselt number (Nu) is calculated based on average hydraulic diameter. The Nu is defined as:

$$\mathrm{Nu} = \frac{\overline{h}\overline{D_h}}{k_{water}} \tag{25}$$

where, $\bar{h}$ is the average heat transfer coefficient, considered as [24]:

$$\overline{h} = \frac{q_w}{\left(T_w - \left(\frac{T_{l,bulk} + T_{u,bulk}}{2}\right)\right)} \tag{26}$$

where, T_w is the average bottom wall temperature, $T_{l,bulk}$ and $T_{u,bulk}$ are the bulk mean temperature of lower and upper fluid domain. $\overline{D_h}$ is the mean hydraulic diameter, defined as:

$$\overline{D_h} = \frac{D_{h,in} + D_{h,out}}{2} \tag{27}$$

where, $D_{h,in}$ and $D_{h,out}$ are the hydraulic diameter of the channel at inlet and outlet respectively. The fluid flow performance is evaluated by using Euler number (Eu) [24]:

$$\mathrm{Eu} = \frac{\left(\Delta p_{lower} + \Delta p_{upper}\right)}{u_{in}^2 \left(\bar{\rho}_{lower} + \bar{\rho}_{upper}\right)} \tag{28}$$

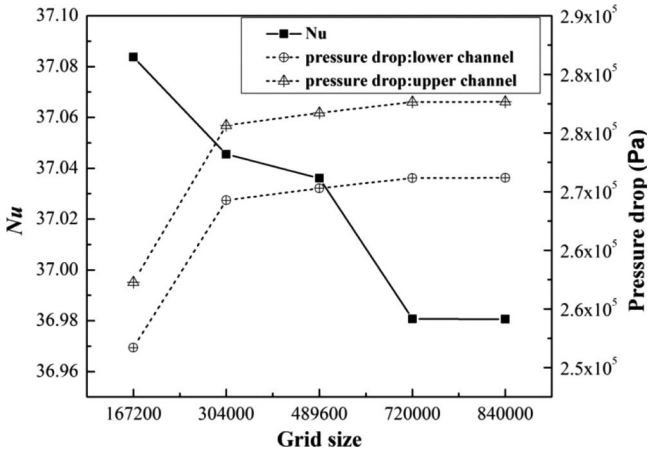

Figure 2. Grid independence test.

where, Δp_{lower} and Δp_{upper} are the pressure drop in lower and upper channel respectively, $\bar{\rho}_{\text{lower}}$ and $\bar{\rho}_{\text{upper}}$ are the mean density of lower and upper fluid domain respectively.

Numerical method

The three-dimensional governing equations are solved numerically using finite-volume based computational fluid dynamics software package, ANSYS FLUENT. The mass, momentum, and energy governing equations are discretized using the second-order upwind scheme. SIMPLE algorithm is used to solve pressure velocity coupled equation and convergence criteria of 10^{-10}, 10^{-12}, and 10^{-15} are used for the convergence of continuity, momentum and energy equation respectively.

Grid independence test

The grid independence test is conducted on computational domain with straight channel to investigate the effect of grid on computational results. In present study, five uniform grid systems are generated with grid size 167,200, 304,000, 489,600, 720,000, and 840,000. In Figure 2, it is found

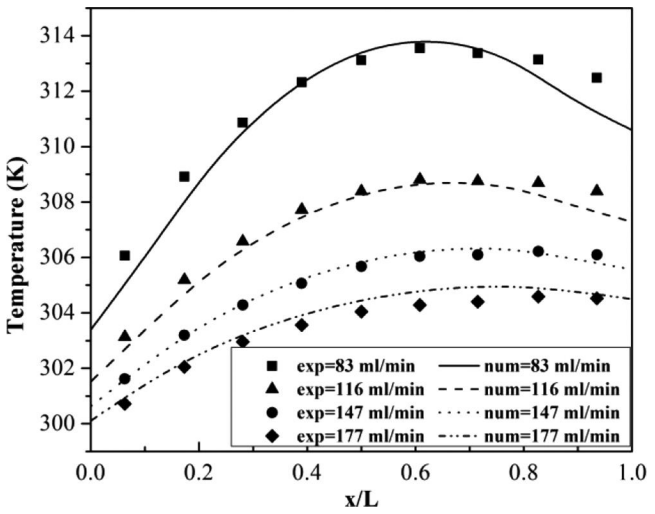

Figure 3. Validation of present numerical model with experimental data by Wei et al. [13].

that variation in values of average Nusselt number, pressure drop in both lower channel and upper channels are very less after grid size 720,000. Hence, grid size 720,000 is used for further simulations.

Validation of present numerical model

For the validation of the present numerical model, the bottom wall temperature, predicted by present numerical model is compared with the experimental data of Wei et al. [13]. Figure 3 compares the temperatures predicted by existing experimental results and present numerical work at four different volume flow rates. From figure, it is found that the present numerical results are in good agreement with experimental data with maximum deviation of 4.2% at the exit for volume flow rates, $Q = 83$ mL min^{-1}.

Results and discussion

Effect of temperature-dependent fluid properties on heat transfer and fluid flow

As reported by Li et al. [38] that the temperature-dependent fluid properties will give much more accurate and close results to actual phenomena for microchannel, in the present work, a comparative study is been performed considering both constant thermal properties and temperature dependent variable properties for DL-MCHS. The constant properties are calculated at inlet temperature of 293 K and the temperature dependent variable properties are described in Eqs. (11)–(14). As the temperature of water increases from inlet to outlet, thermal conductivity of the fluid (k) increases but viscosity (μ) decreases. With the increase in thermal conductivity, heat transfer rate increases. But with the decrease in viscosity of the fluid, flow velocity increases which results in thinning of thermal boundary layer. Thus convective heat transfer coefficient is increased results in increased heat transfer rate. The other two fluid properties, i.e., density (ρ) and specific heat (c_p) do not play significant role in heat transfer as their variations with temperature are very less as compared to k and μ. On the other hand, the effect of temperature dependent fluid properties mainly, ρ and μ on fluid flow characteristics are analyzed by Euler number (Eu). With the rise in temperature of water from inlet to outlet both the density ρ and viscosity μ are decreased. But, the variation of ρ is very less as compared to μ, therefore in fluid flow analysis also, ρ plays insignificant role as compared to μ. The lesser is the viscosity, the lesser will be the frictional losses and hence the pressure drop across the channel becomes less.

Figure 4 shows the variation of ratio of mean Nusselt number based on temperature-dependent property to that of the constant property (Nu_{var}/Nu_{con}) and the variation of ratio of Euler number

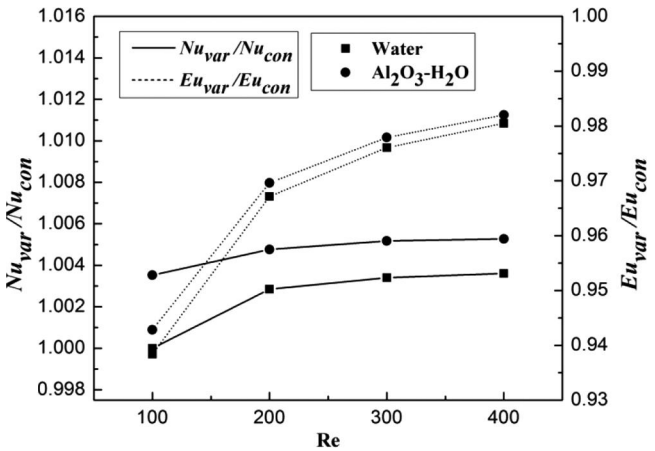

Figure 4. Variation of Nu_{var}/Nu_{con} and Eu_{var}/Eu_{con} with Re for water and Al_2O_3 flowing through straight channel (TF = 1).

using temperature-dependent property by Euler number based on constant property (Eu_{var}/Eu_{con}) with Re for straight DL-MCHS (TF = 1). It is observed that Nu_{var}/Nu_{con} is always greater than one, which means that predicted heat transfer rate using temperature-dependent property is always more than that of using constant fluid property. Also, this ratio increases with the increase in Re. Similarly, the ratio of mean Nusselt number based on temperature-dependent property to that of using constant property (Nu_{var}/Nu_{con}) for Al_2O_3–H_2O nanofluid is also greater than one and this ratio for Al_2O_3–H_2O nanofluid with $\phi = 2\%$ and $d_p = 10$ nm is higher than that of water. Therefore, it can be concluded that the heat transfer characteristics for Al_2O_3–H_2O is more sensitive to temperature-dependent properties as compared to water. It is also observed from Figure 4 that the variation rate of heat transfer considering variable property is marginal at higher Re as compared to lower Re.

It is also observed that Eu_{var}/Eu_{con} is always less than one for both water and Al_2O_3–H_2O ($d_p = 10$ nm and $\phi = 2\%$). This shows that the pressure drop across the channel is lower using temperature-dependent property as compared to constant property. Though the variations for both water and nanofluid are similar but the value of the Eu_{var}/Eu_{con} is smaller for water as compared to Al_2O_3–H_2O for all Re range. Also the effect of variable properties on Eu_{var}/Eu_{con} is more prominent at lower Re.

Effect of tapered channel on heat transfer and fluid flow

Figure 5*a* shows the variation of overall thermal resistance (R_{th}) with Re for various geometries having TF = 1, 0.801, 0.5, and 0.2. It is observed that overall thermal resistance decreases with tapering of channel and with increment in Re. When water flows through the straight channel (TF = 1), the formation of both hydrodynamic and thermal boundary layer take place. The thickness of both the boundary layers increases along the length of the channel. Again convective heat transfer coefficient is inversely proportional to thermal boundary layer thickness [42]. Thus, heat transfer coefficient also decreases along the length of the channel which increases the temperature gradient along the length of the channel. But, in tapered channel (TF < 1) the velocity of water keeps on increasing along the length of the channel due to converging path. Because of this increased velocity, the thermal boundary layer thickness reduces and thus, increases the heat transfer coefficient along the channel length as compared to straight channel. Therefore, overall thermal resistance has been reduced with the improved heat transfer as defined in Eq. (24). Also, with increasing Reynolds number, the flow velocity increases and ultimately overall thermal resistance decreases. From Figure 5*b* similar trend

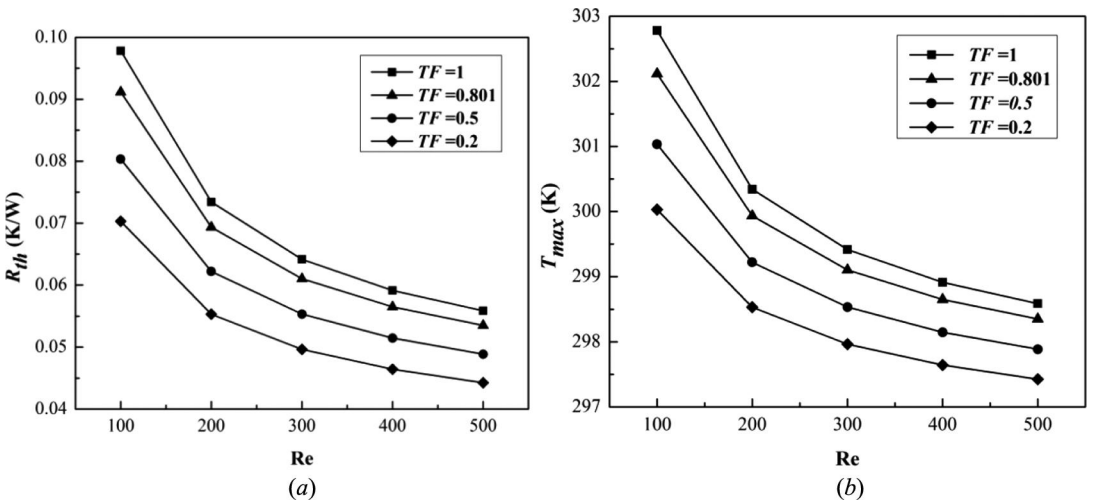

Figure 5. Variation of (*a*) overall thermal resistance (*b*) maximum base temperature with Re for different TF using water as coolant.

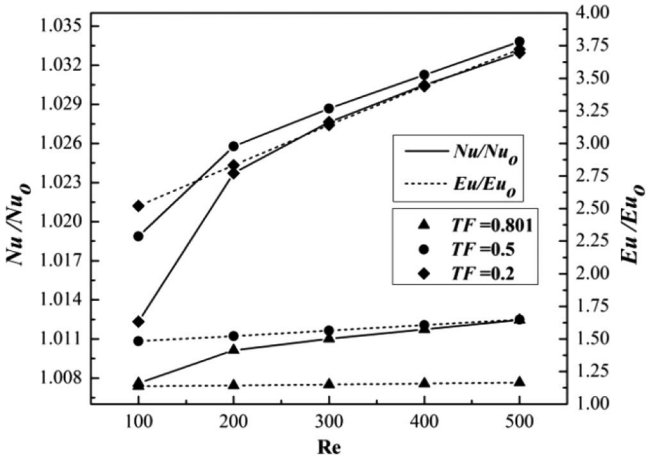

Figure 6. Variation of Nu/Nu_o and Eu/Eu_o with Re for different TF using water as coolant.

of variation is observed for the maximum base temperature (T_{max}) of DL-MCHS with Re for all geometries. The maximum base temperature decreases with increase in Re and with decrease in TF. As overall thermal resistance decreases with the increase in Re and with the decrease in TF, the heat transfer also increases and hence the base temperature is decreased. Finally, it can be concluded that tapered channel gives better thermal performance as compared to straight channel.

Figure 6 shows the variation of Nu/Nu_o (i.e., the ratio of mean Nusselt number with $TF < 1$ to mean Nusselt number with $TF = 1$) with Re for different tapering factors. Thus, the variation of Nu/Nu_o represents the comparison of convective heat transfer of tapered channel with straight channel. It is observed that for all three different tapering factors, the value of Nu/Nu_o is greater than one, which means tapered channel always gives better heat transfer as compared to straight channel. It is also observed that Nu/Nu_o with $TF = 0.2$ is less than that of $TF = 0.5$ for the entire range of Reynolds number considered in the analysis. This means that there is an optimal TF in the range of $0.5 > TF > 0.2$ up to which Nu increases and beyond that Nu starts declining. Figure 7 shows that optimum tapering factor to have maximum heat transfer rate. Figure 6 also shows the variation of Eu/Eu_o with

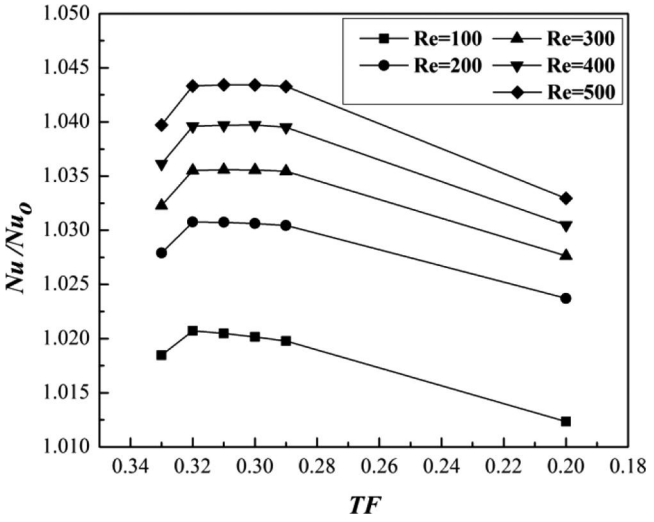

Figure 7. Variation of Nu/Nu_o with TF for different Re using water as coolant.

Re for TF = 0.801, 0.5 and 0.2, and it has been noticed that the value of Eu/Eu_o is greater than one for all tapered channel geometries. Moreover, unlike Nu/Nu_o the value of Eu/Eu_o increases monotonically with the decrease in TF and increase in Re. As higher the value of Euler number, the higher will be pressure drop and hence higher pumping power. So, it is always desirable to have lower Euler number for better flow performance. Therefore, from Figure 6, it is evident that the pressure drop across the channel increases with the tapering of a tapered channel.

If the enhancement of heat transfer is the prime objective, then the geometry of tapered channel can be optimized by taking highest value of Nu/Nu_o. Initially Nu/Nu_o increases with the decrease in TF and attains a maximum value; however, further decrement of TF produces reverse effect. Figure 7 shows the variation of Nu/Nu_o with TF for Re in the range of 100 to 500. It is observed that the highest value of Nu/Nu_o is obtained at TF = 0.32 for Reynolds number in the range of 100 to 200. But for Re = 300, 400, and 500, the highest value of Nu/Nu_o is obtained almost at TF = 0.31 and beyond that decreases. This decrement in Nu/Nu_o clearly indicates that after a particular TF, the convective heat transfer becomes less although Nusselt number for all tapered channel is higher than straight channel.

Effect of tapered channel on overall performance

The overall performance of the system can be evaluated through performance factor (Pf) which is given as

$$Pf = \left(\frac{Nu}{Nu_o}\right)\left(\frac{Eu}{Eu_o}\right)^{-1} \tag{29}$$

Pf will determine whether the design of tapered DL-MCHS is viable or not. Figure 8 shows the variation of Pf with Re for TF = 0.801 to 0.2. It is noticed that the performance factor for all TFs and for all Reynolds number range considered is less than unity. This implies that the overall performance of the tapered channel is lower as compared to straight channel. It is also clear that the thermal performance of DL-MCHS enhances with tapering but at the same time pressure drop also increases. Therefore, it can be concluded that the use of tapered channel is not viable when hydraulic performance is taken into account but when only thermal performance is the prime objective tapered DL-MCHS gives better performance than conventional straight channel.

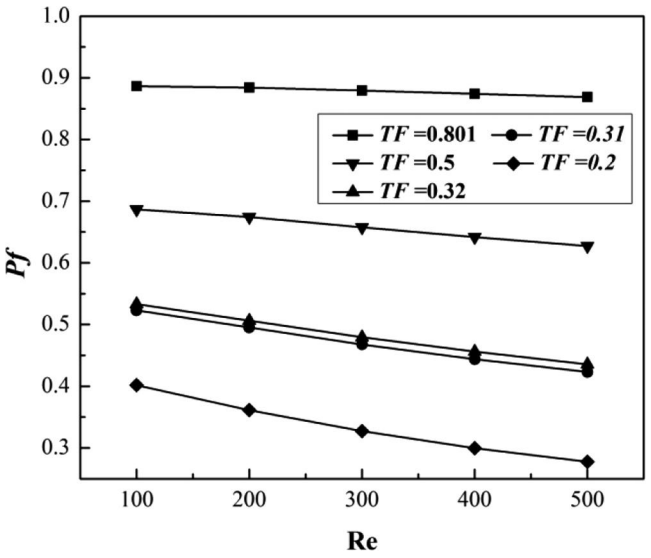

Figure 8. Variation of performance factor for different TF using water as coolant.

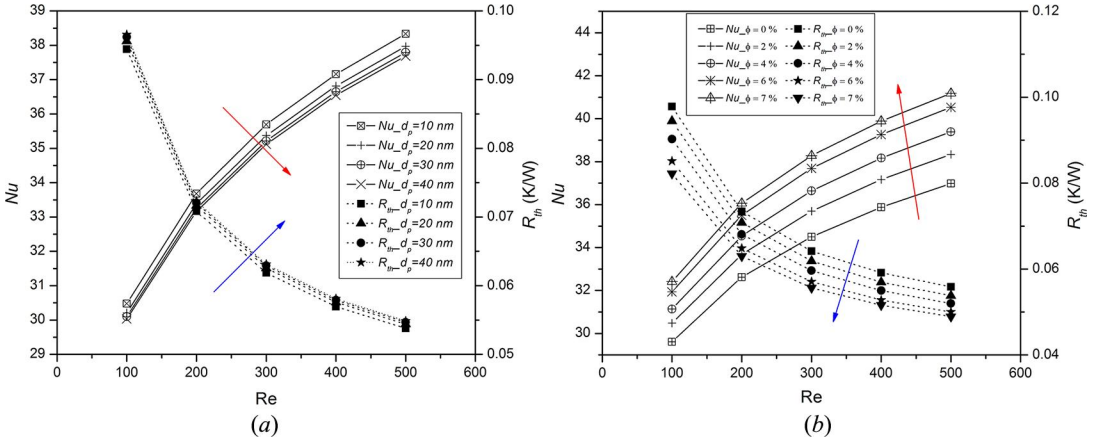

Figure 9. Variation of thermal performance with the effect of (*a*) nanoparticle diameter (*b*) volume fraction.

Performance enhancement using Al_2o_3–H_2o nanofluid

As mentioned earlier, that in the present work Al_2O_3–H_2O nanofluid is used to enhance the performance of tapered DL-MCHS. Based on literature data available, it has been found that nanofluids have a much higher thermal conductivity as compared to thermal conductivity of its base fluid even at very low particle concentration and due to this, the application of nanofluids appears promising in heat transfer augmentation.

Figure 9*a* shows the effect of nanoparticle diameter (d_p) on thermal performance of Al_2O_3–H_2O ($\phi = 2\%$) nanofluid flowing through the straight DL-MCHS (i.e., TF = 1). It is observed that Nu increases and R_{th} decreases with the decrease in nanoparticle diameter. The reason behind the enhancement of thermal performance is the increase in surface area to volume ratio with the decrease in nanoparticle diameter which consequently increases the thermal conductivity of nanofluid. Two mechanisms namely, Brownian motion of nanoparticle and liquid layering around nanoparticles are also responsible in enhancement of thermal conductivity of nanofluids [43]. Table 3 shows the thermal conductivity of nanofluids at different diameters and volume fraction. It has been seen in Table 3 that thermal conductivity is highest for Al_2O_3–H_2O having $d_p = 10$ nm for volume concentration of 0.02 to 0.07. Thus, maximum enhancement of thermal performance can be obtained with $d_p = 10$ nm. Hence Al_2O_3–H_2O nanofluid with $d_p = 10$ nm is used for further simulation in the present study. Figure 9*b* shows the effect of nanoparticle volume concentration on thermal performance of Al_2O_3–H_2O ($d_p = 10$ nm) nanofluid flowing through straight DL-MCHS (TF = 1). Different volume fractions have been taken to compare thermal performance where $\phi = 0\%$ stands for pure water. It is observed that Nu increases and R_{th} decreases with the increase in volume concentration. For the entire Reynolds number range considered in the analysis, the highest Nu and the lowest R_{th} are found with the volume fraction 7%. This may be due to increase in thermal conductivity with the increase in volume fraction of nanofluid as metal oxides have higher thermal conductivity than the base fluid as depicted in Table 3. From the table, it has also been identified that $\phi = 7\%$ gives highest thermal performance and hence it is used for further simulation.

Table 3. Thermal conductivity (k) of Al_2O_3–H_2O nanofluid in W m^{-1} K^{-1} at various volume fraction and particle diameters.

ϕ	$d_p = 10$ nm	$d_p = 20$ nm	$d_p = 30$ nm	$d_p = 40$ nm
2%	0.6613223	0.6467025	0.6398518	0.6356227
4%	0.6963459	0.6732454	0.6624209	0.6557385
6%	0.7256181	0.6954296	0.6812837	0.6725510
7%	0.7389699	0.7055484	0.6898875	0.6802196

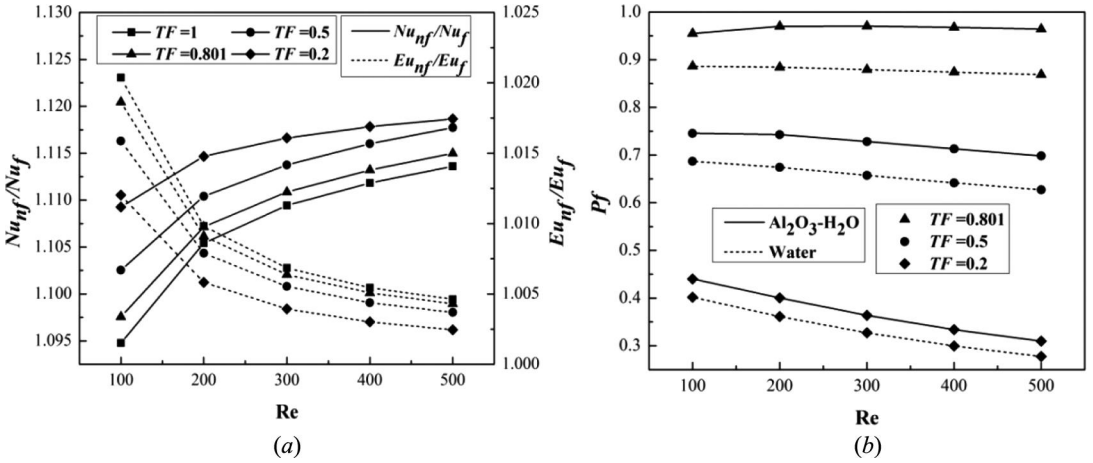

Figure 10. Variation of (*a*) Nu_{nf}/Nu_f and Eu_{nf}/Eu_f (*b*) performance factor with Re for water and nanofluid (Al_2O_3–H_2O) ($\phi = 7\%$) at different TFs.

Effect on thermal performance of tapered DL-MCHS using nanofluid

Figure 10*a* represents the comparison of mean Nusselt number of nanofluid with mean Nusselt number of water (Nu_{nf}/Nu_f) with Re for different tapering factors. Al_2O_3–H_2O nanofluid with $d_p = 10$ nm and $\phi = 7\%$ is used as coolant fluid. It has been found that Nu_{nf}/Nu_f is always greater than one for all the geometries and Re range, which means nanofluid gives higher thermal performance than water. Also, the value of Nu_{nf}/Nu_f increases with the decrease in TF and increase in Re. Figure 10*a* also shows the variation of Eu_{nf}/Eu_f with different tapering factors. It is observed that the value of Eu_{nf}/Eu_f is greater than one for all geometries and Re, which means nanofluid results in higher pressure drop than water. The reason behind this is higher viscosity of nanofluid as compared to water due to inclusion of nanoparticles. The viscosity of nanofluid increases with the increase in volume concentration of nanoparticle. Therefore, it can be concluded that nanofluids enhance the thermal performance with an increase in pressure drop penalty.

Thus to predict the overall performance of tapered DL-MCHS using nanofluid, the performance factor of nanofluid is compared with the performance factor of water. The performance factor for nanofluid is given by

$$Pf_{nf} = \left(\frac{Nu_{nf}}{Nu_o}\right)\left(\frac{Eu_{nf}}{Eu_o}\right)^{-1} \tag{30}$$

where, Nu_{nf} indicates the mean Nusselt number using nanofluid for any channel; Nu_o is the mean Nusselt number for straight DL-MCHS (TF = 1) using water; Eu_{nf} is Euler number using nanofluid for any channel and Eu_o is Euler number for straight DL-MCHS (TF = 1) using water. Figure 10*b* shows the variation of performance factor with Al_2O_3–H_2O ($\phi = 7\%$) and water for different tapering factors of 0.801, 0.5, and 0.2. It is interestingly observed that the performance factor is less than one for both nanofluid and water though performance factor using nanofluid is higher than that for water for all different tapering factors. This shows that, though the overall performance of nanofluid is higher than water but still even using nanofluid as coolant, tapered DL-MCHS is not advantageous from the perspective of overall performance. However, from thermal performance point of view only, use of tapered DL-MCHS with nanofluid as working fluid can be very much effective.

Conclusion

A novel tapered DL-MCHS with converging lower and upper channel is investigated with counter flow of both water and Al_2O_3–H_2O nanofluid and is compared with conventional straight DL-MCHS.

The effect of the tapered channel on the maximum base temperature, overall thermal resistance, average Nusselt number and Euler number has been investigated numerically where temperature-dependent thermo-physical properties are used for both the fluids and the following conclusions are made:

- Temperature dependent fluid properties like thermal conductivity and viscosity plays dominant role on heat transfer but in determining fluid flow characteristics only viscosity plays dominant role. The other properties like density and specific heat play insignificant role as their variation with temperature is very less than that of thermal conductivity and viscosity.
- Temperature dependent fluid properties predict higher heat transfer and lower pressure drop. It is also found that the effect of the temperature-dependent fluid properties on the heat transfer is more in Al_2O_3–H_2O than water while the effect of temperature-dependent properties in the fluid flow is more in water than Al_2O_3–H_2O.
- Tapered DL-MCHS gives better thermal performance than the straight DL-MCHS but with a penalty of increased pumping power with the decrease in TF.
- The value of Nu/Nu_o increases with the decrease in TF up to 0.32 for the Reynolds number range 100 to 200, while for Reynolds number range of 300 to 500, Nu/Nu_o starts decreasing after TF = 0.31. Also, Eu/Eu_o increases with the decrease in TF and increase in Re. Thus, more the tapering factor higher is the pumping power.
- The thermal performance of the DL-MCHS increases with the decrease in nanoparticle diameter and with the increase in nanoparticle volume concentration. The values of the Nu_{nf}/Nu_f and Eu_{nf}/Eu_f are greater than one for the range of Reynolds number and all tapering factors considered in the analysis. Therefore, use of nanofluid as coolant gives better performance than water with a drawback of increase in pumping power.
- From overall performance point of view, it is not advantageous to use tapered channel. Even if Al_2O_3 nanofluid is used, the performance factor is less than unity, though thermal performance is better compared to water.
- When heat dissipation is the main objective, use of tapered DL-MCHS is always effective for all Re range.

References

[1] D. B. Tuckerman and R. F. W. Pease, "High-performance heat sinking for VLSI," *IEEE Electron Device Lett.*, vol. 2, pp. 126–129, 1981. DOI: 10.1109/edl.1981.25367.

[2] T. M Adams, S. I. Abdel-Khalik, S. M. Jeter, and Z. H. Qureshis, "An experimental investigation of single-phase forced convection in microchannels," *Int. J. Heat Mass Transfer*, vol. 41, pp. 851–857, 1997. DOI: 10.1016/s0017-9310(97)00180-4.

[3] K. C Toh, X. Y. Chen, and J. C. Chai, "Numerical computation of fluid flow and heat transfer in microchannels," *Int. J. Heat Mass Transfer*, vol. 45, pp. 5133–5141, 2002. DOI: 10.1016/s0017-9310(02)00223-5.

[4] O. Mokrani, B. Bourouga, C. Castelain, and H. Peerhossaini, "Fluid flow and convective heat transfer in flat microchannels," *Int. J. Heat Mass Transfer*, vol. 52, pp. 1337–1352, 2009. DOI: 10.1016/j.ijheatmasstransfer.2008.08.022.

[5] J. Li, G. P. Peterson, and P. Cheng, "Three-dimensional analysis of heat transfer in a micro-heat sink with single phase flow," *Int. J. Heat Mass Transfer*, vol. 47, pp. 4215–4231, 2004. DOI: 10.1016/j.ijheatmasstransfer.2004.04.018.

[6] W. Qu and I. Mudawar, "Analysis of three-dimensional heat transfer in micro-channel heat sinks," *Int. J. Heat Mass Transfer*, vol. 45, pp. 3973–3985, 2002. DOI: 10.1016/s0017-9310(02)00101-1.

[7] W. Qu and I. Mudawar, "Experimental and numerical study of pressure drop and heat transfer in a single-phase micro-channel heat sink," *Int. J. Heat Mass Transfer*, vol. 45, pp. 2549–2565, 2002. DOI: 10.1016/s0017-9310(01)00337-4.

[8] K. Vafai and L. Zhu, "Analysis of two layered micro channel heat sink concept in electronic cooling," *Int. J. Heat Mass Transfer*, vol. 42, pp. 2287–2297, 1999. DOI: 10.1016/s0017-9310(98)00017-9.

[9] D. Sharma, H. Garg, and P. P. Bajpai, "Performance comparison of single and double layer microchannel using liquid metal coolants: A numerical study," *ARME*, vol. 1, no. 2, pp. 9–17, 2012.

[10] S. L Beh, K. K. Tio, G. A. Quadir, and K. N. Seetharamu, "Fast transient solution of a two-layered counter-flow microchannel heat sink," *Int. J. Numer. Methods Heat Fluid Flow*, vol. 19, pp. 595–616, 2009. DOI: 10.1108/09615530910963544.

[11] C. Leng, X. Wang, and T. Wang, "An improved design of double-layered microchannel heat sink with truncated top channels," *Appl. Therm. Eng.*, vol. 79, pp. 54–62, 2015. DOI: 10.1016/j.applthermaleng.2015.01.015.
[12] J. M Wu, J. Y. Zhao, and K. J. Tseng, "Parametric study on the performance of double-layered microchannels heat sink," *Energy Convers. Manage.*, vol. 80, pp. 550–560, 2014. DOI: 10.1016/j.enconman.2014.01.014.
[13] X. Wei, Y. Joshi, and M. K. Patterson, "Experimental and numerical study of a stacked microchannel heat sink for liquid cooling of microelectronic devices," *J. Heat Transfer*, vol. 129, pp. 1432–1444, 2007. DOI: 10.1115/1.2754781.
[14] M. K. Patterson, X. Wei, Y. Joshi, and R. Prasher, "Numerical study of conjugate heat transfer in stacked microchannels," IEEE Conference Publications, The Ninth Intersociety Conf. on Thermal and Thermomechanical Phenomena in Electronic Systems (IEEE Cat. No.04CH37543), IEEE, Las Vegas, NV, USA, vol. 1, 2004, pp. 372–380.
[15] A. K. M. M. Morshed and J. A. Khan, "Numerical analysis of single phase multi layered microchannel heat sink with inter-connects between vertical channels," Proc. 14th Int. Heat Transf. Conf. Washington, DC, USA, vol. 6, 2010, pp. 133–140.
[16] P. Skandakumaran, A. Ortega, T. Jamal-Eddine, and R. Vaidyanathan, "Multi-layered sic microchannel heat sinks-modeling and experiment," IEEE Conference Publications, The Ninth Intersociety Conf. on Thermal and Thermomechanical Phenomena in Electronic Systems (IEEE Cat. No.04CH37543), IEEE, Las Vegas, NV, USA, vol. 1, 2004, pp. 352–360.
[17] M Hatami and D. D. Ganji, "Thermal and flow analysis of microchannel heat sink (MCHS) cooled by Cu–water nanofluid using porous media approach and least square method," *Energy Convers. Manage.*, vol. 78, pp. 347–358, 2004. DOI: 10.1016/j.enconman.2013.10.063.
[18] C. J Ho, L. C. Wei, and Z. W. Li, "An experimental investigation of forced convective cooling performance of a microchannel heat sink with Al_2O_3/water nanofluid," *Appl. Therm. Eng.*, vol. 30, pp. 96–103, 2010. DOI: 10.1016/j.applthermaleng.2009.07.003.
[19] S. M Peyghambarzadeh, S. H. Hashemabadi, A. R. Chabi, and M. Salimi, "Performance of water based CuO and Al_2O_3 nanofluids in a Cu–Be alloy heat sink with rectangular microchannels," *Energy Convers. Manage.*, vol. 86, pp. 28–38, 2014. DOI: 10.1016/j.enconman.2014.05.013.
[20] T. Tsai and R. Chein, "Performance analysis of nanofluid-cooled microchannel heat sinks," *Int. J. Heat Fluid Flow*, vol. 28, pp. 1013–1026, 2007. DOI: 10.1016/j.ijheatfluidflow.2007.01.007.
[21] A. Sakanova, S. Yin, J. Zhao, J. M. Wu, and K. C. Leong, "Optimization and comparison of double-layer and double-side micro-channel heat sinks with nano fluid for power electronics cooling," *Appl. Therm. Eng.*, vol. 65, pp. 124–134, 2014. DOI: 10.1016/j.applthermaleng.2014.01.005.
[22] H. E. Ahmed, M. I. Ahmed, I. M. F. Seder, and B. H. Salman, "Experimental investigation for sequential triangular double-layered microchannel heat sink with nano fluids," *Int. Commun. Heat Mass Transfer*, vol. 77, pp. 104–115, 2016. DOI: 10.1016/j.icheatmasstransfer.2016.06.010.
[23] T. Hung and W. Yan, "Enhancement of thermal performance in double-layered microchannel heat sink with nanofluids," *Int. J. Heat Mass Transfer*, vol. 55, pp. 3225–3238, 2012. DOI: 10.1016/j.ijheatmasstransfer.2012.02.057.
[24] B. Rajabifar, "Enhancement of the performance of a double layered microchannel heatsink using PCM slurry and nanofluid coolants," *Int. J. Heat Mass Transfer*, vol. 88, pp. 627–635, 2015. DOI: 10.1016/j.ijheatmasstransfer.2015.05.007.
[25] M. R. Gorji, O. Pourmehran, M. Hatami, and D. D. Ganji, "Statistical optimization of microchannel heat sink (MCHS) geometry cooled by different nanofluids using RSM analysis," *Eur. Phys. J. Plus*, vol. 130, no. 2, pp. 22, 2015. DOI: 10.1140/epjp/i2015-15022-8.
[26] X. Wang, B. An, L. Lin, and D. Lee, "Inverse geometric optimization for geometry of nano fluid-cooled microchannel heat sink," *Appl. Therm. Eng.*, vol. 55, pp. 87–94, 2013. DOI: 10.1016/j.applthermaleng.2013.03.010.
[27] T. W. Ting, Y. M. Hung, and N. Guo, "Effects of streamwise conduction on thermal performance of nanofluid flow in microchannel heat sinks," *Energy Convers. Manage.*, vol. 78, pp. 14–23, 2014. DOI: 10.1016/j.enconman.2013.10.061.
[28] Y. L. Zhai, G. D. Xia, X. F. Liu, and Y. F. Li, "Heat transfer enhancement of Al_2O_3-H_2O nanofluids flowing through a micro heat sink with complex structure," *Int. Commun. Heat Mass Transfer*, vol. 66, pp. 158–166, 2015. DOI: 10.1016/j.icheatmasstransfer.2015.05.025.
[29] A. Sakanova, C. Chun, and J. Zhao, "Performance improvements of microchannel heat sink using wavy channel and nanofluids," *Int. J. Heat Mass Transfer*, vol. 89, pp. 59–74, 2015. DOI: 10.1016/j.ijheatmasstransfer.2015.05.033.
[30] G. Wang, D. Niu, F. Xie, Y. Wang, X. Zhao, and G. Ding, "Experimental and numerical investigation of a microchannel heat sink (MCHS) with micro-scale ribs and grooves for chip cooling," *Appl. Therm. Eng.*, vol. 85, pp. 61–70, 2015. DOI: 10.1016/j.applthermaleng.2015.04.009.
[31] D. D. Ma, G. D. Xia, Y. F. Li, Y. T. Jia, and J. Wang, "Design study of micro heat sink configurations with offset zigzag channel for specific chips geometrics," *Energy Convers. Manage.*, vol. 127, pp. 160–169, 2016. DOI: 10.1016/j.enconman.2016.09.013.

[32] D. Yang, Y. Wang, G. Ding, Z. Jin, J. Zhao, and G. Wang, "Numerical and experimental analysis of cooling performance of single-phase array microchannel heat sinks with different pin-fin configurations," *Appl. Therm. Eng.*, vol. 112, pp. 1547–1556, 2017. DOI: 10.1016/j.applthermaleng.2016.08.211.
[33] T. Hung, T. Sheu, and W. Yan, "Optimal thermal design of microchannel heat sinks with different geometric configurations," *Int. Commun. Heat Mass Transfer*, vol. 39, pp. 1572–1577, 2015. DOI: 10.1016/j.icheatmasstransfer.2012.10.008.
[34] M. Dehghan, M. Daneshipour, M. S. Valipour, R. Rafee, and S. Saedodin, "Enhancing heat transfer in microchannel heat sinks using converging flow passages," *Energy Convers. Manage.*, vol. 92, pp. 244–250, 2015. DOI: 10.1016/j.enconman.2014.12.063.
[35] B. Osanloo, A. M. Amar, A. Solati, and M. Baghani, "Performance enhancement of the double-layered microchannel heat sink by use of tapered channels," *Appl. Therm. Eng.*, vol. 102, pp. 1345–1354, 2016. DOI: 10.1016/j.applthermaleng.2016.04.073.
[36] K. C. Wong and M. L. Ang, "Thermal hydraulic performance of a double-layer microchannel heat sink with channel contraction," *Int. Commun. Heat Mass Transfer*, vol. 92, pp. 269–275, 2016. DOI: 10.1016/j.icheatmasstransfer.2016.09.013.
[37] H. Herwig and S. P. Mahulikar, "Variable property effects in single-phase incompressible flows," *Int. J. Thermal Science*, vol. 45, pp. 977–981, 2006. DOI: 10.1016/j.ijthermalsci.2006.01.002.
[38] Z. Li, X. Huai, Y. Tao, and H. Chen, "Effects of thermal property variations on the liquid flow and heat transfer in microchannel heat sinks," *Appl. Therm. Eng.*, vol. 27, pp. 2803–2814, 2007. DOI: 10.1016/j.applthermaleng.2007.02.007.
[39] L. Chai, G. Dong, and H. Sheng, "Numerical study of laminar flow and heat transfer in microchannel heat sink with offset ribs on sidewalls," *Appl. Therm. Eng.*, vol. 92, pp. 32–41, 2016. DOI: 10.1016/j.applthermaleng.2015.09.071.
[40] J. Buongiorno, "Convective transport in nanofluids," *J. Heat Transfer*, vol. 128, pp. 240–250, 2006. DOI: 10.1115/1.2150834.
[41] M. Corcione, "Empirical correlating equations for predicting the effective thermal conductivity and dynamic viscosity of nanofluids," *Energy Convers. Manage.*, vol. 52, pp. 789–793, 2011. DOI: 10.1016/j.enconman.2010.06.072.
[42] T. L. Bergman, A. S. Lavine, F. P. Incropera, and D. P. Dewitt, *Fundamentals of Heat and Mass Transfer*, 7th ed. New York: Wiley, 2011.
[43] M. Raja, R. Vijayan, P. Dineshkumar, and M. Venkatesan, "Review on nano fluids characterization, heat transfer characteristics and applications," *Renewable Sustainable Energy Rev.*, vol. 64, pp. 163–173, 2016. DOI: 10.1016/j.rser.2016.05.079.